Taxonomic Assessment of the Trinil Molars Using Non-Destructive 3D Structural and Development Analysis

TANYA M. SMITH
Department of Human Evolution, Max Planck Institute for Evolutionary Anthropology, Deutscher Platz 6, D-04103, Leipzig, GERMANY; and Department of Anthropology, 11 Divinity Avenue, Harvard University, Cambridge, MA 02138, USA; tsmith@fas.harvard.edu

ANTHONY J. OLEJNICZAK
Department of Human Evolution, Max Planck Institute for Evolutionary Anthropology, Deutscher Platz 6, D-04103, Leipzig, GERMANY; and Grupo de Antropología Dental, Centro Nacional de Investigación sobre la Evolución Humana, Avda. de la Paz 28, 09004 Burgos, SPAIN; olejniczak@eva.mpg.de

KORNELIUS KUPCZIK
Department of Human Evolution, Max Planck Institute for Evolutionary Anthropology, Deutscher Platz 6, D-04103, Leipzig, GERMANY; kornelius.kupczik@eva.mpg.de

VINCENT LAZZARI
Department of Human Evolution, Max Planck Institute for Evolutionary Anthropology, Deutscher Platz 6, D-04103, Leipzig, GERMANY; and Steinmann-Institut für Geologie, Mineralogie und Paläontologie, Nußallee 8, 53115 Bonn, GERMANY; and European Synchrotron Radiation Facility, 6 rue ules Horowitz, BP 220, 38043 Grenoble cedex, FRANCE; screetch20100@yahoo.fr

JOHN DE VOS
Department of Palaeontology, Nationaal Natuurhistorisch Museum Naturalis, P.O. Box 9517, NL-2300 RA Leiden, THE NETHERLANDS; vos@naturalis.nnm.nl

OTTMAR KULLMER
Department of Paleoanthropology and Messel Research, Senckenberg Research Institute, D-60325 Frankfurt a.M., GERMANY; ottmar.kullmer@senckenberg.de

FRIEDEMANN SCHRENK
Department of Vertebrate Paleontology, Institute for Ecology, Evolution, and Diversity, Johann Wolfgang Goethe University, Frankfurt a.M., GERMANY; schrenk@malawi.net

JEAN-JACQUES HUBLIN
Department of Human Evolution, Max Planck Institute for Evolutionary Anthropology, Deutscher Platz 6, D-04103, Leipzig, GERMANY; hublin@eva.mpg.de

TEUKU JACOB‡
Department of Bioanthropology and Palaeoanthropology, Faculty of Medicin, Gadjah Mada University, Yogyakarta, INDONESIA

PAUL TAFFOREAU
European Synchrotron Radiation Facility, 6 rue ules Horowitz, BP 220, 38043 Grenoble cedex, FRANCE; paul.tafforeau@esrf.fr

‡*deceased.*

ABSTRACT

Two molars recovered at Trinil, Java, have been the subject of more than a century of debate since their discovery by Eugène Dubois in 1891–92. These molars have been attributed to several ape and human taxa (including *Pan* and *Meganthropus*), although most studies agree that they are either fossil *Pongo* or *Homo erectus* molars. Complicating the assessment of these molars is the metric and morphological similarity of *Pongo* and *Homo erectus* molars, and uncertainty regarding their serial positions within the maxillary row. Here we applied non-destructive conventional and synchrotron microtomographic imaging to measure the structure of these molars and aspects of their development. Comparisons were made with modern *Homo* and *Pongo* maxillary molars, as well as small samples of fossil *Pongo* and *Homo erectus* molars. Root spread was calculated from three-dimensional surface models, and enamel thickness and enamel-dentine junction morphology were assessed from virtual planes of section. Developmental features were investigated using phase contrast X-ray synchrotron imaging.

 © 2009 PaleoAnthropology Society. All rights reserved. **ISSN 1545-0031**

The highly splayed root morphology of the Trinil maxillary molars suggests that they are not third or fourth molars. Trinil molar enamel thickness is most similar to *Homo sapiens* and *Homo erectus* first molar mean values, and is thicker than most modern *Pongo* molars. The shapes of their enamel-dentine junctions are outside the *Pongo* range of variation, and within the range of variation in *Homo*. Moreover, the internal long-period line periodicity of these two teeth is most similar to fossil and extant hominins, and is outside of the known range of fossil and living *Pongo*. Taken together, these results strongly suggest that the two molars are in fact *Homo erectus* teeth, and Dubois' original attribution to "*Pithecanthropus erectus*" (a junior synonym of *Homo erectus*) is correct.

INTRODUCTION

During 1891 and 1892 excavations in Trinil, Java, Eugène Dubois recovered several fossils that he attributed to the new hominin taxon "*Pithecanthropus erectus*" (Dubois 1892, 1894, 1896). Dubois' assertion that these fossils represented a missing link between apes and humans, and the intense international debate that followed, helped to establish the field of paleoanthropology (Shipman and Storm 2002; de Vos 2004). Opinions about the skullcap, femur, and molars were varied around the turn-of-the-century, although the teeth received less attention (Hooijer 1948). Groesbeek (1996) reviewed at length the history of taxonomic assessments of the molars, which is briefly discussed here. Dubois (1894, 1896) considered the two teeth to belong to one individual of "*P. erectus*." Hooijer (1948) attributed the teeth to a "peculiar" fossil orangutan individual after comparison with the massive collection of Sumatran fossil orangutans recovered by Dubois. Von Koenigswald also attributed the teeth to a fossil orangutan in his initial assessment, but later assigned them to the new hominin genus "*Meganthropus*" (von Koenigswald 1967). Most recently, Schwartz and Tattersall (2003) suggested that these two molars "were probably not hominid," although they included the lesser-known premolar with their description of the remaining Trinil hominin material.

Dubois (1894, 1896) originally identified the two molars as a right upper third molar (11620) and a heavily worn left upper second molar (11621) (Figure 1). While he was convinced that they represented a hominin, he also noted that the highly splayed roots were not found in living human molars, suggesting that the Trinil individual was intermediate between living humans and apes. Hooijer (1948) noted that these root angles were not greater than that found in one of the Sumatran fossil orangutans recovered by Dubois, and argued that the teeth represented an upper fourth molar (11620) and an upper third molar (11621). He justified this attribution by arguing that fourth molars made up approximately 1.5% of more than 1,000 isolated fossil orangutan molars, and 1.3% of several hundred molars from recent orangutan skulls that he had examined. Lavelle and Moore (1973) reported an even higher incidence of supernumerary molars (2% maxillary, 4% mandibular) in 100 orangutan skulls.

The taxonomic discrimination of Asian hominoid faunas is particularly difficult due to convergence in tooth structure and size between *Pongo* and *Homo*, as well as overlap in tooth size between large *Pongo* and small *Gigantopithecus* from the Asian mainland (reviewed by Ciochon et al. 1996; Demeter et al. 2004). The aim of the research presented here is to assess the structure and development of the two enigmatic Trinil molars to determine their taxonomic affiliation using modern non-destructive techniques.

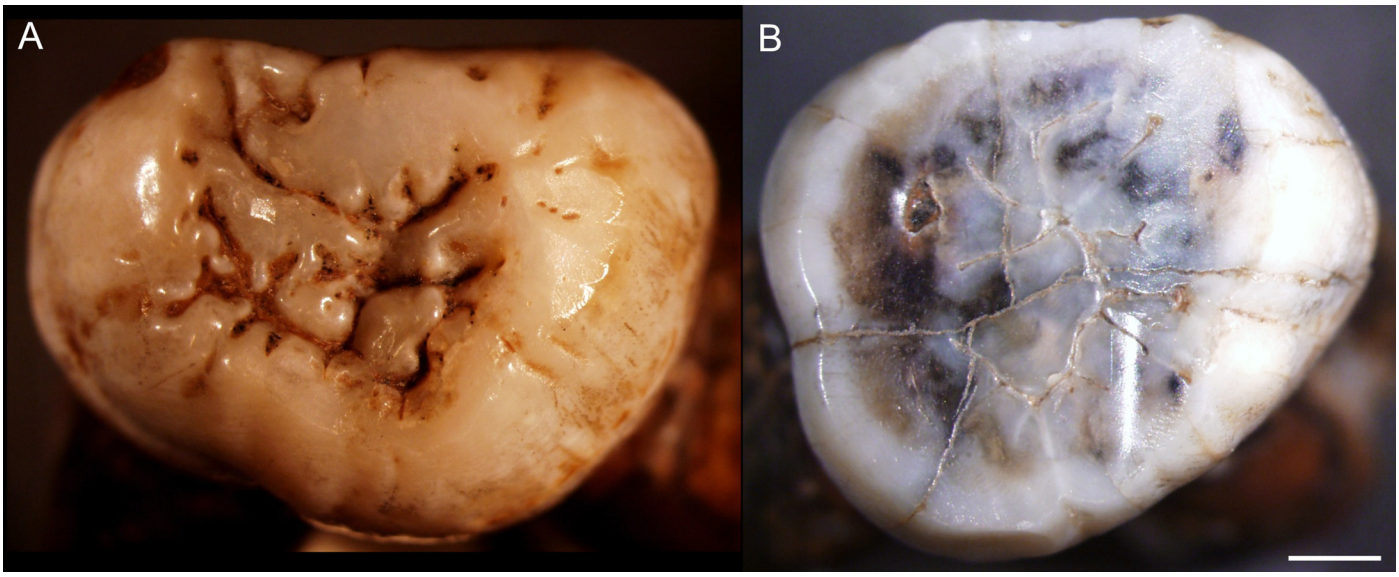

Figure 1. The Trinil molars crowns: A) 11620, B) 11621. The scale is equal to 2 mm.

To assess the serial positions and taxonomy of the Trinil molars, we collected data on root structure, enamel thickness, enamel-dentine junction (EDJ) shape, and enamel development. While some measurements are known to overlap between modern humans and orangutans (e.g., enamel thickness: Martin 1985; Olejniczak et al. 2008a; Smith 2007; Smith et al. 2006; crown formation time: Smith 2007), it is likely that a combination of structural and developmental features will yield better taxonomic resolution than analyses based on single variables. Ultimately, we seek to identify a suite of characters that may be used to resolve the composition of mixed Asian Pleistocene faunas (e.g., Longgupo Cave, central China: reviewed in Wang et al. 2007; "Chinese Apothecary" material: von Koenigswald 1935, 1952; Tham Khuyen Cave, northern Vietnam: Ciochon et al. 1996; Mohui Cave, southern China: Wang et al. 2007; Sangiran Dome, Java, Indonesia: Grine and Franzen 1994). Resolution of these ambiguous mixed-taxon faunas will provide important insight into the biogeography and ecology of these Asian hominoids, particularly *Homo erectus* (e.g., "*Pithecanthropus*," "*Meganthropus*," "*Sinanthropus*").

MATERIALS AND METHODS

The Trinil molars were photographed, molded with Coltene President impression materials, and cast with Epo-Tek 301 resin. Both teeth show enamel growth disruptions (hypoplasias) in the imbricational enamel; 11620 shows a linear hypoplasia slightly higher in the cervical enamel than 11621. The enamel of both teeth was missing around the majority of the circumference of the cervical margin, prohibiting complete counts of external growth lines (perikymata). A distal interproximal facet was observed on 11621 but not on 11620.

The teeth were scanned using a Skyscan 1172 microtomographic system (microCT; housed at the Max Planck Institute for Evolutionary Anthropology, Leipzig, Germany) at 100 kV, 100 mA, with an aluminum-copper filter and an isometric voxel size of 15.13 microns. Unfortunately, due to diagenetic remineralization of the teeth (see Olejniczak and Grine 2006; Smith and Tafforeau 2008; Tafforeau et al. 2006), it was not possible to distinguish the interface between enamel and dentine in the entirety of the cross-sectional slice data. It was possible, however, to model the external surface of the teeth (discussed below). The teeth were subsequently scanned on beamline ID 19 at the European Synchrotron Radiation Facility (Grenoble, France) using several different optical configurations designed to reveal overall tooth structure and fine microstructure. This included absorption mode scans with an isotropic voxel size of 31.12 microns at an energy of 60 keV, long distance propagation phase contrast scans with a voxel size of 4.96 microns at 51 keV and 5 meters of propagation, and high resolution propagation phase contrast scans with a voxel size of 0.7 microns at 52 keV using a multilayer monochromator and propagation distances of 150 and 300 mm (Smith et al. 2007a; Tafforeau et al. 2006; Tafforeau and Smith 2008).

ROOT STRUCTURE

The two Trinil molars were compared to eight maxillary molars from Pleistocene sediments of the Sangiran Dome (Java, Indonesia) and the Lida Ajer cave (Sumatra, Indonesia) (Table 1) (Grine and Franzen 1994; Hooijer 1948; Tyler 2001). Four of these teeth have been attributed to *Homo erectus* and two to *Pongo pygmaeus sumatrensis*, and in two cases the taxonomic affiliation remains unresolved (either *H. erectus* or *Pongo*). The modern comparative sample comprises maxillary first, second, and third molars of *Homo sapiens* (n=35; made available by the Oral Biology Department at the University of Newcastle-upon-Tyne) and *Pongo pygmaeus* (n=16; housed at the Museum für Naturkunde der Humboldt-Universität, Berlin; Department of Cell and Developmental Biology, University College London, UK; and Royal College of Surgeons of England, UK). The *H. erectus* and fossil *Pongo* molars from Sangiran were scanned with the Skyscan microCT. The comparative *H. sapiens* and *P. pygmaeus* sample was scanned on a medical CT scanner (housed at the Hammersmith Hospital, London) and on a microCT system (housed at the Bundesanstalt für Materialforschung und -prüfung, Berlin).

Amira imaging software (v. 4.1.2, Mercury Computer Systems) was employed to render 3D visualizations of the molars and to take angular measurements, as detailed in Kupczik (2003). The spread between the palatal (lingual) and buccal molar roots was quantified as follows (Figure 2): a best fit plane was defined by up to 10 points at the enamel-cementum junction (cervical plane); the tooth was then positioned to show the largest extension of bucco-palatal (BP) root splay; the tooth was then projected onto a Cartesian reference plane and angles were measured between the long axis of the palatal and buccal roots, respectively, and an axis perpendicular to the cervical plane. The bucco-palatal root angle, representing the sum of palatal and buccal root deviation, was measured from both the mesial and distal aspects, and an average was calculated. In the case of curved roots or root tips, the line was projected onto the cervical two-thirds of the long axis of the root.

ENAMEL THICKNESS AND ENAMEL-DENTINE JUNCTION SHAPE

Due to the extensive diagenesis of the molars it was not possible to record 3D measurements of enamel thickness (*sensu* Kono 2004; Olejniczak et al. 2008a, b; Tafforeau 2004), nor 3D EDJ morphology (e.g., Skinner et al. 2008; Tafforeau 2004), so a cross-sectional approach was taken. Mesial section overviews of the Trinil molars were made through the cusp tips and dentine horns from synchrotron microtomographs at 31.12 micron resolution using OsiriX DICOM visualization and measurement software (Rosset et al. 2004) and VG Studio MAX 1.2.1 and 2.0 (Volume Graphics, Heidelberg, Germany) (Figure 3). Figure 4 depicts the variables quantified on each section using a digitizing tablet interfaced with SigmaScan software (SPSS Science, Inc.): the total area of the tooth crown section (a, mm^2), the area of the coronal dentine enclosed by the enamel cap (b, mm^2), the area of the enamel cap (c, mm^2), and the length of the EDJ

TABLE 1. FOSSIL SAMPLE OF MAXILLARY MOLARS USED FOR THE COMPARISON OF ROOT SPLAY.

Taxon	Specimen accession number	Molar position	Collection[1]
H. erectus/Pongo ?	11620	??	DBC
	11621	??	DBC
	S7-17	RM^1	SMF
	S16	RM^2	Yogyakarta
H. erectus	S7-37	RM^1	SMF
	S27	RM^1	Yogyakarta
	S27	RM^2	Yogyakarta
	S11-DIJ2	LM^3	Yogyakarta
P. pygmaeus sumatrensis	11573-226	LM^1	DBC
	11573-226	LM^2	DBC

[1] DBC=Dubois Collection, Nationaal Natuurhistorisch Museum, Leiden; Yogyakarta= Gadjah Mada University, Yogyakarta; SMF=Senckenberg Forschungsinstitut und Naturmuseum, Frankfurt.

(e, mm). Following Martin (1983, 1985), average enamel thickness (AET) is calculated as [c/e], yielding the average linear distance (mm units), or thickness, from the EDJ to the outer enamel surface. Relative enamel thickness (RET) is calculated as [100 * AET / $\sqrt{b}$], a unitless measure of enamel thickness suitable for inter-taxon comparisons. Estimates of worn enamel for 11621 were based on the morphology of the crown of 11620 as well as the curvature of the remaining lateral enamel. The chipped cervical enamel of the 11621 protocone was similarly estimated. These values were compared with previously published maxillary molar data on modern *Homo* (n=113) and *Pongo* (n=19) (Smith et al. 2005, 2006). Enamel thickness also was quantified for virtual mesial sections of two *Homo erectus* teeth from the Chinese Apothecary Collections (von Koenigswald 1935, 1952) housed at the Senckenberg Forschungsinstitut und Naturmuseum, Frankfurt, which were scanned on the Skyscan microCT.

Molar EDJ morphology was quantified in the Trinil and Chinese *Homo erectus* mesial sections by collecting nine landmarks and semi-landmarks in each section (following Olejniczak et al. 2004, 2007; see Figure 4), and calculating a series of relative distances from these landmarks. These relative distances were combined with a database of homologous maxillary measurements representing recent taxa (Olejniczak et al. 2007; Smith et al. 2006): *Pongo* (n=31), *Homo* (n=115), *Gorilla* (n=9), and *Pan* (n=7). The relative distances were subjected to discriminant function analysis (DFA) using SPSS software (v. 12.0, SPSS, Inc.). The Trinil and Chinese *Homo erectus* molars were treated as ungrouped cases in the DFA, and the sample size of each taxon was not used to adjust the probability of molars belonging to any group (for a discussion of prior probabilities see e.g., Tabachnick and Fidel 2000). It has been demonstrated elsewhere that metameric variation in mesial cross-section EDJ shape is minimal and does not overwhelm the ability of this technique to distinguish taxa (Olejniczak et al. 2007). Moreover, as the Trinil molars are of uncertain position within the dental arcade (Groesbeek 1996), molars from all three maxillary positions were combined in the analysis.

ENAMEL DEVELOPMENT

To assess internal developmental features, small portions of the mid-lateral and cervical enamel of both teeth were scanned using an isotropic 0.7 micron voxel size with propagation phase contrast X-ray synchrotron micro-CT. This technique facilitates non-destructive resolution of dental microstructure at the sub-micron level (Tafforeau 2004; Tafforeau et al. 2006), including the long-period line periodicity (Smith et al. 2007a; Tafforeau and Smith 2008). Strong ring artifacts due to the multilayer and detector were corrected using conditional flatfield correction (where the beam reference is used depending on the sample absorption), residual horizontal line removal, subtraction of a filtered average of all scan projections (general ring correction), and finally a correction of residual rings on reconstructed slices (adapted from Tafforeau 2004). Because the diagenetic pattern reduced the visibility of incremental lines, a specific processing tool was applied to selectively enhance the visibility of the incremental lines slice by slice in the 3D volumes. Virtual histological slices were then prepared using average projections on a virtual thickness of 40 slices

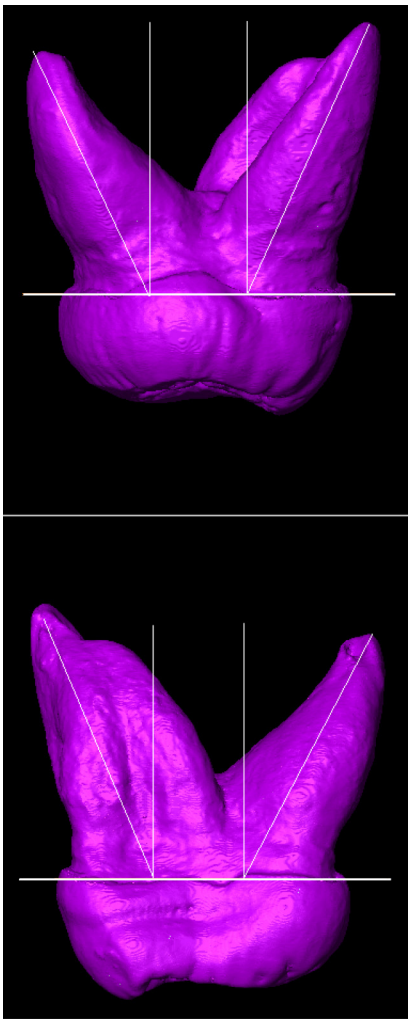

Figure 2. Measurement of bucco-palatal root spread in maxillary molar 11620: top is distal view, bottom is mesial view. The horizontal line indicates the cervical plane projected onto a Cartesian reference plane. Root splay was measured from the angle between the long axis of the palatal and buccal roots, respectively, and an axis perpendicular to the cervical plane.

(28 microns) after precise alignment along incremental features, following the protocol described in Tafforeau et al. (2007) and Tafforeau and Smith (2008).

RESULTS

ROOT STRUCTURE

Tables 2 and 3 and Figure 5 demonstrate that both *H. sapiens* and *P. pygmaeus* overlap in the degree of root spread for all maxillary molar positions. There is a decreasing mesial-to-distal gradient in buccal-palatal root splay in both taxa. Upper third molars in *H. sapiens* have near-parallel converging roots (i.e., the BP angle is negative), or fully coalesced roots. Single teeth of *H. erectus* (S27) show very large first and second molar root spreads that exceed those of modern humans, while third molar roots (S11-DIJ2) are coalesced similar to the condition in modern humans (Table 3). Among the taxonomically unresolved specimens, S7-17 (M^1) has a very small root spread compared to S16 (M^2). The root spreads of the Trinil molars are markedly different from those of the third molars among the comparative sample, and are most comparable to the maximum values found for first and second molars of *H. erectus* and *P. pygmaeus*. In contrast to the compressed crown morphology highlighted in earlier diagnoses, the marked root splay found in this study suggests that these are unlikely to be third or fourth molars.

ENAMEL THICKNESS AND ENAMEL-DENTINE JUNCTION SHAPE

The average and relative enamel thicknesses of the Trinil molars and Chinese *Homo erectus* molars are given in Table 4. The value of the lightly worn Trinil molar (11620) was found to be similar to that of the Chinese maxillary first molar (CA 770: type of "*Sinanthropus officinalis*").

Results of the discriminant function analysis of EDJ relative distances show that recent hominoid taxa are grouped reliably based on the nine distance ratios (87% correctly classified; 84% correctly classified in cross-validation). The analysis had three significant functions with a combined X^2 (24) = 263.8, Wilk's $\lambda = 0.182$ ($p < 0.001$). After removal of the first function, there was still a strong association between groups and predictors: X^2 (14) = 71.3, Wilk's $\lambda = 0.631$ ($p < 0.001$). After removal of the second function, the significant relationship between groups and predictors persisted: X^2 (6) = 23.3, Wilk's $\lambda = 0.861$ ($p = 0.001$). A plot of the first two discriminant functions is shown in Figure 6. The first discriminant function accounts for 82.4% of the variance and has a negative relationship with the relative width between dentine horns, and positive relationships with the relative lingual cusp height and the relative buccal cusp height. The second function accounts for 12.2% of the variance and has positive relationships with relative height of the lingual dentine horn, the relative height of the buccal dentine horn, and relative width of the dentine crown at the cusp base. The third function accounted for 5.4% of the variance and has a negative relationship with the relative width of the lingual cusp, and positive relationships with the relative width of the buccal cusp and the relative width of the dentine crown at the midline. Both of the Trinil molars and Chinese *Homo erectus* molars are within the range of variation defined by *Homo*, which is separated from other taxa primarily on function 1 by dentine horns that are relatively closer together and taller cusps relative to the cervical diameter.

ENAMEL DEVELOPMENT

It was not possible to determine the total number of long-period incremental lines in enamel (perikymata/Retzius lines) due to the degree of attrition and missing cervical enamel on both Trinil teeth, prohibiting calculation of the crown formation time. It was possible to image Retzius lines non-destructively, however, which were closely spaced in the lower lateral enamel (Figure 7). In one of the Trinil teeth (11621) the long-period line periodicity was determined to be 6 days (Figure 8). The other tooth (11620) was estimated to be either 6 or 7 days; it was not possible to discern be-

Figure 3. Virtual sections through the mesial cusps of the Trinil molars, showing the planes used to quantify enamel thickness and enamel-dentine shape: A)11620, B) 11621. Note the difference in tissue contrast between the upper sections derived from synchrotron absorption imaging, and the lower sections, which are derived from conventional laboratory microCT imaging (see text for details). The depression in the lateral/cervical enamel of the left cusp (paracone) of 11620 corresponds to the hypoplasia observed on the surface of the tooth crown. The scale is equal to 10 mm.

tween these two values due to slight but consistent ambiguity in the incremental lines.

DISCUSSION

ROOT STRUCTURE

Modern human molars are characterized by a gradual decrease of molar root spread from mesial to distal (i.e., M1>M2>M3) (Kupczik 2003). The large root splay of maxillary first molars is potentially related to the increased lateral excursion of the mandible further anteriorly (Macho and Spears 1999; Spears and Macho 1998). In contrast, third molars have less splayed or even coalesced roots, and are less well adapted to resist non-axial occlusal loads (Spears and Macho 1998). Supernumerary (i.e., fourth) molars often do not develop roots at all, as has been observed in a *Pan troglodytes* individual (Kupczik and Dean 2008). Despite Hooijer's (1948) observation of similarity between the Trinil molars and a Sumatran fossil orangutan specimen,

TABLE 2. MEAN AND STANDARD DEVIATION OF BUCCO-PALATAL ROOT SPLAY IN THE EXTANT COMPARATIVE SAMPLE.

Taxon	M^1	M^2	M^3
H. sapiens	28±7 (n=12)	18±7 (n=12)	13±13 (n=11)
P. pygmaeus	32±13 (n=6)	21±11 (n=5)	19±6 (n=4)

See text for calculation details.

TABLE 3. BUCCO-PALATAL ROOT SPLAY (IN DEGREES) IN THE FOSSIL SAMPLE.

Taxon	Specimen	Molar serial position	BP-root splay
H. erectus/Pongo ?	11620	??	53
	11621	??	44
	S7-17	RM^1	14
	S16	RM^2	42
Homo erectus	S7-37	RM^1	32
	S27	RM^1	47
	S27	RM^2	53
	S11-DIJ2	LM^3	9
P. pygmaeus sumatrensis	11573/226	LM^1	34
	11573/226	LM^2	25

*Figure 4. Schematic of Trinil molar 11620 showing the variables used for quantification of the enamel thickness and enamel-dentine junction shape. The area of the enamel cap is represented as c, the area of the dentine under the enamel cap is represented as b, and the length of the enamel-dentine junction is represented as e. The average enamel thickness (AET) is calculated as (c/e), and relative enamel thickness (RET) is calculated as [(c/e)/√b] * 100. Landmarks are defined as follows: 1) tip of the lingual enamel cervix; 2) lingual intersection of the EDJ and a line parallel to the cervical diameter and bisecting the length between the cervical diameter and landmark 5; 3) lingual intersection of the EDJ and a line parallel to the cervical diameter and running through landmark 5; 4) protocone dentine horn tip; 5) lowest point of the EDJ between the protocone and paracone cusp tips; 6) paracone dentine horn tip; 7) buccal intersection of the EDJ and a line parallel to the cervical diameter and running through landmark 5; 8) buccal intersection of the EDJ and a line parallel to the cervical diameter and bisecting the length between the cervical diameter and landmark 5; and, 9) tip of the buccal enamel cervix. Landmark 1 was made to lie at (0, 0) and landmark 9 at (0, 100) in every specimen examined in order to account for differences in tooth size.*

two molars from this collection (11590/18 and 11591/126) identified as upper fourth molars by Hooijer (1948) have root portions that are partially fused and are not splayed like the two Trinil molars. The extremely splayed root morphology of the Trinil molars therefore suggests that they are unlikely to represent third or fourth upper molars.

ENAMEL THICKNESS AND ENAMEL-DENTINE JUNCTION SHAPE

The relative enamel thickness value for the lightly worn Trinil molar (11620) is most similar to that of a *H. erectus* first molar, in addition to average values for modern human first molars and orangutan third molars (Table 5). Furthermore, the Trinil and Chinese *H. erectus* values are similar to an approximated relative enamel thickness value from a histological section of a *H. erectus* maxillary first molar from Sangiran (Figure 9). These data suggest that enamel thickness in *H. erectus* first maxillary molars is similar to that found in modern *H. sapiens*, and is absolutely and relatively greater than that of *Homo neanderthalensis* (Olejniczak et al. 2008b).

Enamel-dentine junction shape in the Trinil molars strongly indicates that these two molars belong to *Homo* rather than to *Pongo*. Previous researchers have found that EDJ shape may be useful in phylogenetic and taxonomic studies due to its conservative morphology relative to the outer enamel surface, and because the EDJ may be measured in molars that are otherwise too worn for trait analysis (e.g., Corruccini 1987; Korenhof 1961; Kraus 1952; Olejniczak et al. 2004, 2007; Sakai and Hanamura 1973; Skinner et al. 2008; Tafforeau 2004). The shape of the EDJ in molar cross-sections differs significantly between primate species

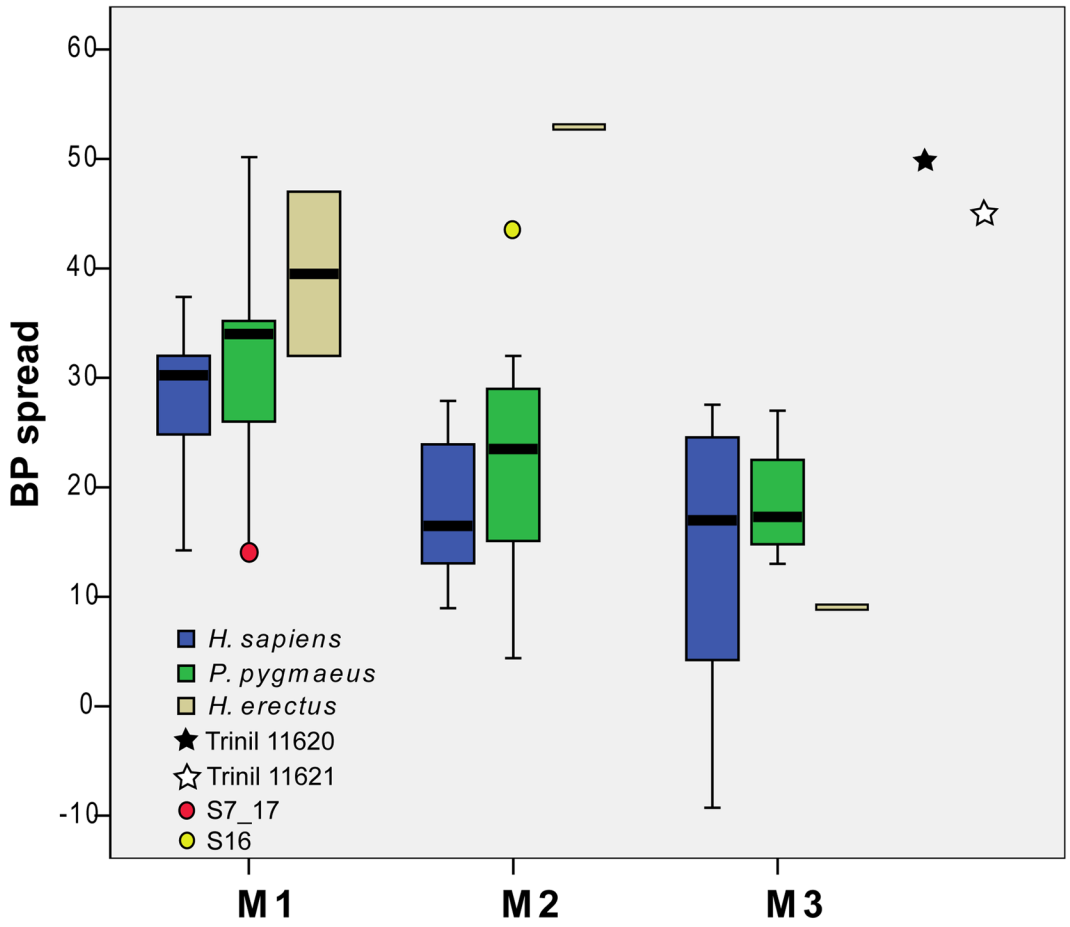

Figure 5. Box and whisker plots of root spread in the modern comparative and fossil sample. Note the root spread of Trinil 11620 and 11621 (stars in the upper right) relative to M1/M2 values for H. erectus *and* P. pygmaeus.

TABLE 4. AVERAGE AND RELATIVE ENAMEL THICKNESS IN THE TRINIL AND CHINESE *HOMO ERECTUS* MOLARS.

Tooth	Type	b (mm²)	c (mm²)	e (mm)	AET	RET
11620	??	52.07	28.98	21.48	1.35	18.69
11621	??	39.75	~25.05	20.26	~1.24	~19.61
CA 770	RUM1	52.43	31.17	23.55	1.32	18.28
CA 771	RUM1/2	59.06	30.12	24.87	1.21	15.76

Variable: b: area of dentine enclosed by the enamel cap; c: area of the enamel cap; e: length of the enamel-dentine junction; AET: average enamel thickness (c/e); RET: relative enamel thickness (([c/e]/ √b) * 100).
~ Approximation derived from reconstruction of the worn enamel crown based on the morphology of the unworn 11620 crown.

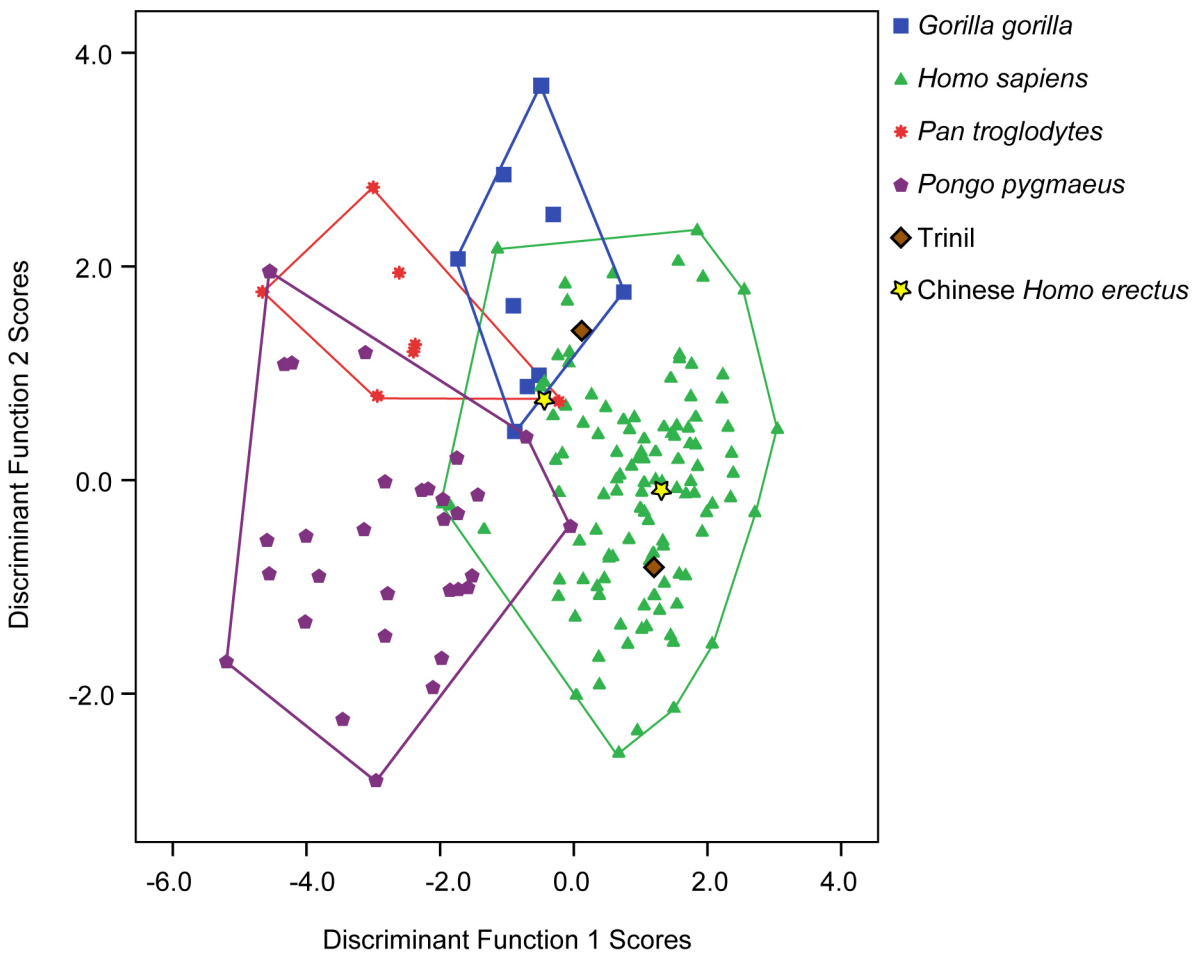

Figure 6. Plot depicting scores on the first two discriminant functions resulting from the DFA of maxillary molar EDJ shape metrics. Overall, 87% of molars were classified correctly (84% in cross-validation). The Trinil molars fall within the range of Homo sapiens *molars and are outside the range of* Pongo *molars. Chinese* Homo erectus *molars also fall within the* Homo sapiens *range. Both Trinil molars were classified as* Homo sapiens *by the DFA when left as ungrouped cases.*

TABLE 5. AVERAGE RELATIVE ENAMEL THICKNESS IN MESIAL MOLAR SECTIONS OF LIVING ORANGUTAN AND HUMAN MAXILLARY MOLARS.

Taxon	M1 (n, range)	M2 (n, range)	M3 (n, range)
Pongo pygmaeus	13.5 (9, 9.9–16.3)	16.2 (6, 11.6–18.1)	18.1 (4, 15.3–19.9)
Homo sapiens	18.8 (37, 14.0–23.9)	21.6 (25, 16.5–28.0)	21.8 (51, 17.0–30.0)

Data from Smith et al. (2005, 2006).

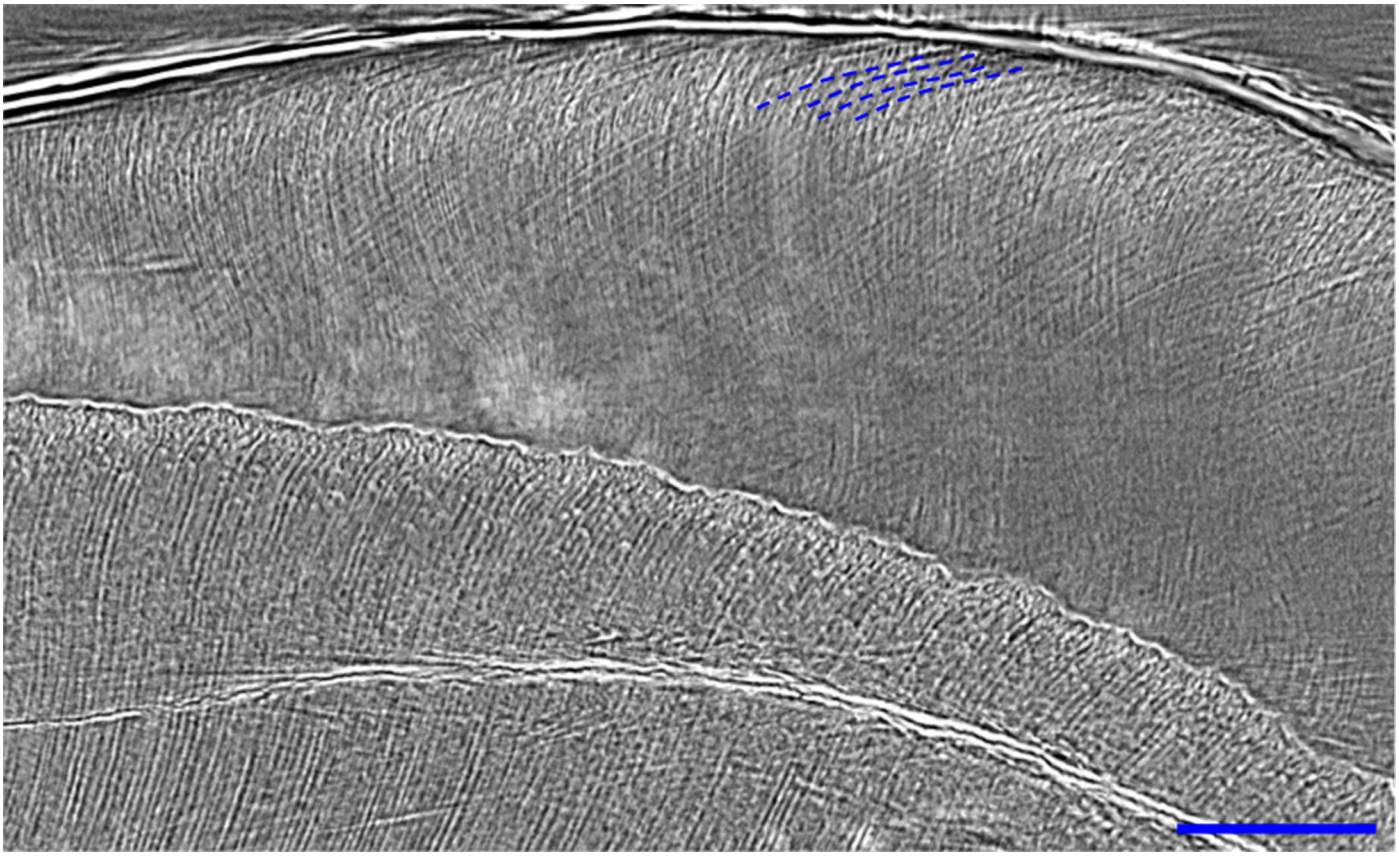

Figure 7. Phase contrast synchrotron microtomographic image showing closely spaced Retzius lines (blue dotted lines) in the lateral enamel of 11620. The enamel surface is at the top of the image, and the cervix is to the left of the image. The virtual section is 28 microns thick (40 slices at 0.7 micron voxel size), and scale bar is equal to 200 microns.

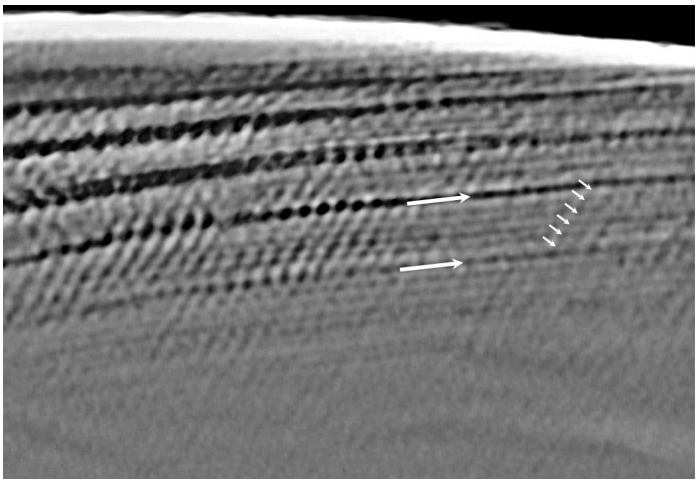

Figure 8. Phase contrast synchrotron microtomographic image showing the long-period line periodicity of the Trinil molar 11621: 6 daily cross-striations (light and dark bands to the right of the small white arrows) can be seen between long-period Retzius lines (larger white arrows).

Figure 9. Histological section of Sangiran S7-37 Homo erectus *upper first molar from Dean et al. (2001). The relative enamel thickness was approximately 17.6, although this value is likely slightly overestimated due to minor section obliquity. Note the similarity in enamel-dentine junction shape with the Trinil upper molars. The scale is equal to 5 mm. Section prepared by Christopher Dean.*

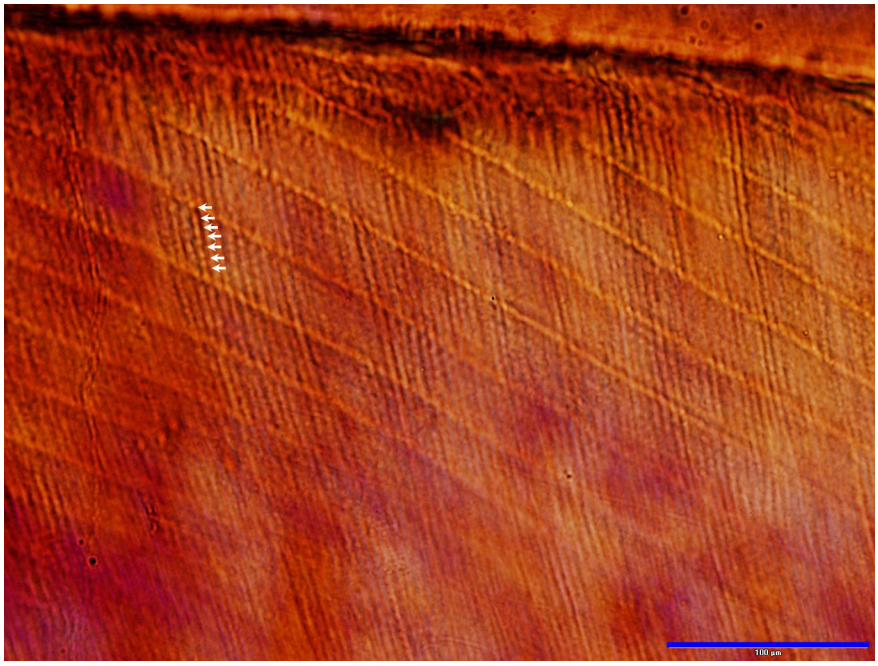

Figure 10. Retzius line periodicity in Homo erectus *S7-37 from Sangiran: seven cross-striations (white arrows) can be seen between pairs of Retzius lines (running diagonally). The scale is equal to 100 microns. Section prepared by Christopher Dean.*

and genera, and overall cross-sectional shape differences also are useful for distinguishing primates at higher levels of classification (Olejniczak et al. 2004, 2007). The present analysis confirms that measurements of the EDJ are a useful tool for taxonomic discrimination, and that significant differences between *Homo* and *Pongo* may be measured, even in worn specimens, from mixed-species assemblages where taxonomic resolution is difficult to ascertain based on external crown morphology.

ENAMEL DEVELOPMENT

Dean et al. (2001) reported a crown formation time for the mesiobuccal cusp of a *H. erectus* upper first molar (S7-37) of 2.5 years. It was not possible to assess crown formation times in the Trinil molars due to missing cervical enamel and attrition. The long-period line periodicity in Plio-Pleistocene fossil hominins ranges from 6 to 9 days, with a mean of approximately 7 days for taxa predating Neanderthals (reviewed in Lacruz et al. 2008; Smith 2008). Modern human long-period line periodicity ranges from 6 to 12 days with a mean of 8.3 days (Smith et al. 2007b). In contrast, fossil orangutans typically show values of 9 days (n=4, Smith and Zhao unpublished data), similar to that of living orangutans (mean=9.5 days, n=24, range=8 to 11 days: Schwartz et al. 2001). Finding a long-period line periodicity of 6 to 7 days in the Trinil molars therefore strongly suggests that these are hominin molars. This argument is strengthened by the observed 7 day long-period line periodicity of a single *H. erectus* individual from Sangiran (Figure 10) (Lacruz et al. 2008).

Long-period line periodicity is known to be the same value within all teeth belonging to an individual, but often varies among individuals (FitzGerald 1998). We were unable to determine if the two teeth are derived from different individuals due to ambiguity in the long-period line periodicity of 11620. Should it be the case that it was 7 days, this would prove that the teeth were derived from two individuals, as the periodicity of 11621 was 6 days. Alternatively, a value of 6 days for both 1160 and 11621 would imply either that the two teeth were derived from a single individual, or possibly from two individuals with identical periodicities.

CONCLUSIONS

The attribution of the Trinil molars to *Homo erectus* advocated by the current study is consistent with the hominin attribution of the other fossil material (skullcap, femur, premolar) recovered from Trinil (reviewed in de Vos 2004). The serial position of these teeth in the maxillary molar row remains unresolved, although our analysis suggests it is unlikely that they represent third or fourth molars. Our assignment of the Trinil molars to *H. erectus* is further supported by a consideration of the other fauna present at the site of Trinil, which indicate a more open environment than the cave localities that have yielded the rich fossil orangutan assemblages (de Vos 1985). The data presented in this study demonstrate that internal crown morphology and development, notably enamel-dentine junction shape and long-period line periodicity, facilitate the distinction of isolated molar remains in mixed-taxa Asian hominoid assemblages where taxonomic attributions have been problematic based on external crown morphology.

ACKNOWLEDGEMENTS

We thank the ESRF ID-19 beamline staff, Bernhard Illerhaus, Matt Skinner, Fred Spoor, Heiko Temming, and staff

at the Hammersmith Hospital for scanning assistance. Diana Carstens, Chris Dean, Frieder Mayer, Don Reid, Silke Streiber, Hendrik Turni, Darlene Weston, and Reinier van Zelst assisted with the acquisition of material, in addition to the Museum für Naturkunde der Humboldt-Universität (Berlin), National Museum of Natural History (Leiden), The Royal College of Surgeons of England (London), and the Senckenberg Research Institute (Frankfurt). Lingxia Zhao is thanked for the use of unpublished data. This study was funded by the European Synchrotron Radiation Facility, the European Virtual Anthropology Network, the Leverhulme Trust, and the Max Planck Society.

REFERENCES

Ciochon, R.L., Long, V.T., Larick, R., Gonzalez, L., Grün, R., De Vos, J., Yonge, C., Taylor, L., Yoshida, H., Reagan, M., 1996. Dated co-occurrence of *Homo erectus* and *Gigantopithecus* from Tham Khuyen Cave, Vietnam. *Proc. Natl. Acad. Sci. USA* 93, 3016–3020.

Corruccini, R.S., 1987. The dentinoenamel junction in primates. I*nt. J. Primatol.* 8, 99–114.

Dean, M.C., Leakey, M.G., Reid, D.J., Schrenk, F., Schwartz, G.T., Stringer, C., Walker, A., 2001. Growth processes in teeth distinguish modern humans from *Homo erectus* and earlier hominins. *Nature* 414, 628–631.

Demeter, F., Bacon, A.M., Nguyen, K.T., Long, V.T., Matsumura, H., Ha, H.N., Schuster, M., Nguyen, M.H., Coppens, Y., 2004. An archaic *Homo* molar from Northern Vietnam. *Curr. Anthropol.* 45, 535–541.

Dubois, E., 1892. Palaeontologische onderzoekingen op Java. *Extra bijvoegsel der Javasche Courant, Verslag van het Mijnwezen over het 3e kwartaal* 1891, 12–14.

Dubois, E., 1894. *Pithecanthropus erectus, einen menschenaehnliche Uebergangsform aus Java*. Landesdruckerei, Batavia.

Dubois, E., 1896. *Pithecanthropus erectus*, einen menschenaehnliche Uebergangsform. In: *Compte-rendu des séances du troisième Congrès International de Zoologie, Leyde, 16-21 Septembre, 1895.* E.J. Brill, Leiden, pp. 251–271, pl. 2.

FitzGerald, C.M., 1998. Do enamel microstructures have regular time dependency? Conclusions from the literature and a large-scale study. *J. Hum. Evol.* 35, 371–386.

Grine, F., Franzen, J.L., 1994. Fossil hominid teeth from the Sangiran Dome (Java, Indonesia). *Courier Forschungsinstitut Senckenberg* 171, 75–103.

Groesbeek, B.J., 1996. The serial position of the Trinil upper molars. *Anthropol. Sci.* 104, 107–130.

Hooijer, D.A., 1948. Prehistoric teeth of Man and of the orang-utan from central Sumatra, with notes on the fossil orang-utan from Java and Southern China. *Zoologische Mededelingen Museum Leiden* 29, 175–301.

Koenigswald, G.H.R. von, 1935. Eine fossile Säugetierfauna mit *Simia* aus Südchina. *Proc. Sect. Sci., K. Akad. Wetensch. Amsterdam* 38, 872–879.

Koenigswald, G.H.R. von, 1952. *Gigantopithecus blacki* VON KOENIGSWALD, a giant fossil hominoid from the Pleistocene of southern China. *Anthropol. Papers Am. Mus. Nat. Hist.*, 43, 310–325.

Koenigswald, G.H.R. von, 1967. De *Pithecanthropus*-kiezen uit de collectie Dubois. *Kon Ned. Ak. v. Wet. A'dam, Verslag van de gewone vergadering der Afd. Natuurkunde* 76, 42–45.

Kono, R., 2004. Molar enamel thickness and distribution patterns in extant great apes and humans: new insights based on a 3-dimensional whole crown perspective. *Anthropol. Sci.* 112, 121–146.

Korenhof, C.A.W., 1961. The enamel-dentine border: a new morphological factor in the study of the (human) molar pattern. P*roc. Koninklijke Nederlands* 64B, 639–664.

Kraus, B.S., 1952. Morphologic relationships between enamel and dentine surfaces of lower first molar teeth. *J. Dent. Res.* 31, 248–256.

Kupczik, K., 2003. *Tooth root morphology in primates and carnivores*. Ph.D. Dissertation, University of London.

Kupczik, K., Dean, M.C., 2008. Comparative observations on the tooth root morphology of *Gigantopithecus blacki*. *J. Hum. Evol.* 54, 196–204.

Lacruz, R.S., Dean, M.C., Ramirez-Rozzi, F., Bromage, T. 2008. Megadontia, striae periodicity and patterns of enamel secretion in Plio-Pleistocene fossil hominins. *J. Anat.* 213, 148–158.

Lavelle, C.L.B., Moore, W.J., 1973. The incidence of agenesis and polygenesis in the primate dentition. *Am. J. Phys. Anthropol.* 38, 671–680.

Macho, G.A., Spears, I.R., 1999. Effects of loading on the biomechanical behavior of molars of *Homo*, *Pan*, and *Pongo*. *Am. J. Phys. Anthropol.* 109, 211–227.

Martin, L.B., 1983. *Relationships of the later Miocene Hominoidea*. Ph.D. Dissertation, University College London.

Martin, L.B., 1985. Significance of enamel thickness in hominoid evolution. *Nature* 314, 260–263.

Olejniczak, A.J., Gilbert, C.C., Martin, L.B., Smith, T.M., Ulhaas, L., Grine, F.E., 2007. Morphology of the enamel-dentine junction in sections of anthropoid primate maxillary molars. *J. Hum. Evol.* 53, 292–301.

Olejniczak, A.J., Grine, F.E., 2006. Assessment of the accuracy of dental enamel thickness measurements using micro-focal X-ray computed tomography. *Anat. Rec.* 288A, 263–275.

Olejniczak, A.J., Martin, L.B., Ulhaas, L., 2004. Quantification of dentine shape in anthropoid primates. *Ann. Anat.* 186, 479–485.

Olejniczak, A.J., Smith, T.M., Feeney, R.N.M., Macchiarelli, R., Mazurier, A., Bondioli, L., Rosas, A., Fortea, J., de la Rasilla, M., García-Tabernero, A., Radovčić, J., Skinner, M.M., Toussaint, M., Hublin, J.-J. 2008b. Dental tissue proportions and enamel thickness in Neandertal and modern human molars. *J. Hum. Evol.* 55, 12–23.

Olejniczak, A.J., Smith, T.M., Wang, W., Potts, R., Ciochon, R., Kullmer, O., Schrenk, F., Hublin, J-J., 2008a. Molar enamel thickness and dentine horn height in *Gigantopithecus blacki*. *Am. J. Phys. Anthropol.* 135, 85–91.

Rosset, A., Spadola, L., Ratib, O., 2004. OsiriX: an open-source software for navigating in multidimensional

DICOM images. *J. Digit. Imaging* 17, 205–216.
Sakai, T., Hanamura, H., 1973. A morphological study of enamel-dentin border on the Japanese dentition: VI. Mandibular molar. *J. Anthropol. Soc. Nippon* 81, 25–45.
Schwartz, G.T., Reid, D.J., Dean, C., 2001. Developmental aspects of sexual dimorphism in hominoid canines. *Int. J. Primatol.* 22, 837–860.
Schwartz. J.H., Tattersall, I. 2003. *The Human Fossil Record*, Volume Two. Wiley-Liss, New York.
Shipman, P., Storm, P., 2002. Missing links: Eugène Dubois and the origins of paleoanthropology. *Evol. Anthropol.* 11, 108–116.
Skinner, M.M., Wood, B.A., Boesch, C., Olejniczak, A.J., Rosas, A., Smith, T.M., Hublin, J.-J., 2008. Dental trait expression at the enamel-dentine junction of lower molars in extant and fossil hominoids. *J. Hum. Evol.* 54, 173–186.
Smith, T.M., 2007. Molar crown development in wild orangutans. *Am. J. phys. Anthropol. Suppl.* 44, 222.
Smith, T.M., 2008. Incremental dental development: methods and applications in hominoid evolutionary studies. *J. Hum. Evol.* 54, 205–224.
Smith, T.M., Olejniczak, A.J., Martin, L.B., Reid, D.J., 2005. Variation in hominoid molar enamel thickness. *J. Hum. Evol.* 48, 575–592.
Smith, T.M., Olejniczak, A.J., Reid, D.J., Ferrell, R.J., Hublin, J.-J., 2006. Modern human molar enamel thickness and enamel-dentine junction shape. *Arch. Oral Biol.* 51, 974–995.
Smith, T.M., Reid, D.J., Dean, M.C., Olejniczak, A.J., Ferrell, R.J., Martin, L.B., 2007b. New perspectives on chimpanzee and human dental development. In: Bailey, S.E., Hublin, J.-J. (Eds.), *Dental Perspectives on Human Evolution: State of the Art Research in Dental Paleoanthropology*. Springer, Dordrecht, pp. 177–192.
Smith, T.M., Tafforeau, P., 2008. New visions of dental tissue research: tooth development, chemistry, and structure. *Evol. Anthropol.* 17, 213–226.
Smith, T.M., Tafforeau, P.T., Reid, D.J., Grün, R., Eggins, S., Boutakiout, M., Hublin, J.-J., 2007a. Earliest evidence of modern human life history in North African early *Homo sapiens*. *Proc. Natl. Acad. Sci. U.S.A.* 104, 6128–6133.
Spears, I.R., Macho, G.A., 1998. Biomechanical behaviour of modern human molars: implications for interpreting the fossil record. *Am. J. Phys. Anthropol.* 106, 467–482.
Tabachnick, B.G., Fidell, L.S., 2000. *Using Multivariate Statistics*. Allyn and Bacon, Boston.
Tafforeau, P., 2004. *Phylogenetic and functional aspects of tooth enamel microstructure and three-dimensional structure of modern and fossil primate molars*. Ph.D. Dissertation, Université de Montpellier II.
Tafforeau, P., Bentaleb, I., Jaeger, J.-J., Martin, C., 2007. Nature of laminations and mineralization in rhinoceros enamel using histology and X-ray synchrotron microtomography: potential implications for palaeoenvironmental isotopic studies. *Palaeogeogr. Palaeoclimatol. Palaeoecol.* 246, 206–227.
Tafforeau, P., Boistel, R., Boller, E., Bravin, A., Brunet, M., Chaimanee, Y., Cloetens, P., Feist, M., Hoszowska, J., Jaeger, J.-J., Kay, R.F., Lazzari, V., Marivaux, L., Nel, A., Nemoz, C., Thibault, X., Vignaud, P., Zabler, S., 2006. Applications of X-ray synchrotron microtomography for non-destructive 3D studies of paleontological specimens. *Appl. Phys. A* 83, 195–202.
Tafforeau, P., Smith, T.M., 2008. Nondestructive imaging of hominoid dental microstructure using phase contrast X-ray synchrotron microtomography. *J. Hum. Evol.* 54, 272–278.
Tyler, D.E., 2001. "*Meganthropus*" cranial fossils from Java. *J. Hum. Evol.* 16, 81–101.
Vos, J. de. 1985. Faunal stratigraphy and correlation of the Indonesian hominid sites. In: Delson, E. (ed.), *Ancestors: The Hard Evidence*, Alan R. Liss, New York, pp. 215–220.
Vos, J. de. 2004. The Dubois collection: a new look at an old collection. In: Winkler Prins, C.F. and Donovan, S.K. (eds.), VII International Symposium 'Cultural Heritage in Geosciences, Mining and Metallurgy: Libraries - Archives - Museums': "Museums and their collections", Leiden (The Netherlands), 19-23 May 2003. *Scripta Geologic, Special Issue* 4, 267–285.
Wang, W., Potts, R., Baoyin, Y., Huang, W., Cheng, H., Edwards, R.L., Ditchfield, P. 2007. Sequence of mammalian fossils, including hominoid teeth, from the Bubing Basin caves, South China. *J. Hum. Evol.* 52, 370–379.